Non-rigid Registration of Pre-procedural MR Images with Intra-procedural Unenhanced CT Images for Improved Targeting of Tumors During Liver Radiofrequency Ablations

N. Archip, S. Tatli, P. Morrison, F. Jolesz, S.K. Warfield, and S. Silverman

Abstract. In the United States, unenhanced CT is currently the most common imaging modality used to guide percutaneous biopsy and tumor ablation. The majority of liver tumors such as hepatocellular carcinomas are visible on contrast-enhanced CT or MRI obtained prior to the procedure. Yet, these tumors may not be visible or may have poor margin conspicuity on unenhanced CT images acquired during the procedure. Non-rigid registration has been used to align images accurately, even in the presence of organ motion. However, to date, it has not been used clinically for radiofrequency ablation (RFA), since it requires significant computational infrastructure and often these methods are not sufficient robust. We have already introduced a novel finite element based method (FEM) that is demonstrated to achieve good accuracy and robustness for the problem of brain shift in neurosurgery. In this current study, we adapt it to fuse pre-procedural MRI with intra-procedural CT of liver. We also compare its performance with conventional rigid registration and two non-rigid registration methods: b-spline and demons on 13 retrospective datasets from patients that underwent RFA at our institution. FEM non-rigid registration technique was significantly better than rigid ($p<10-5$), non-rigid b-spline ($p<10-4$) and demons ($p<10-4$) registration techniques. The results of our study indicate that this novel technology may be used to optimize placement of RF applicator during CT-guided ablations.

Keywords: non-rigid registration, biomechanical model, b-splines, demons, radiofrequency ablation, targeting.

1 Introduction

In the last decade, percutaneous image guided tumor ablations techniques such as radiofrequency (RF) ablation and cryoablation have become an alternative minimally invasive method to treat primary and metastatic liver malignancies in select groups of patients. In particular, radiofrequency ablation has emerged as effective and practical [1], particularly in tumors smaller than 3 cm in diameter.

CT is the most common imaging modality used to guide biopsy and tumor ablation procedures. Typically, unenhanced CT images are obtained intermittently to plan the procedure, guide biopsy needle and ablation applicator placement, and to monitor the ablation. Contrast agent may be administered only once during CT-guided

N. Ayache, S. Ourselin, A. Maeder (Eds.): MICCAI 2007, Part II, LNCS 4792, pp. 969–977, 2007.

intervention. The most of liver tumors are visible on contrast-enhanced CT or MRI obtained prior to the procedure. However, these tumors are either invisible or not demonstrated optimally on unenhanced CT images obtained during the procedure. This may increase the procedure time, and/or lead to non-diagnostic cytopathologic assessment, requiring repeat biopsy or sub-optimal ablation applicator placement. Particularly in percutaneous ablations, accurate applicator placement has a direct impact on treatment outcome since the location of the applicator has a certain effect range and suboptimal applicator placement ultimately results in an inadequate ablation (Figure 1).

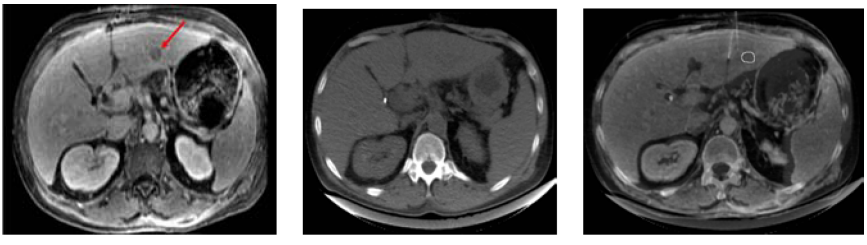

(a) (b) (c)

Fig. 1. Current RFA procedure. Patient with hepatocellular carcinoma of the left hepatic lobe. The patient was a poor surgical candidate due to other co-morbidities and underwent RFA under CT guidance. (a) The tumor margin can be clearly seen on the pre-procedural MRI. (b) The intra-procedural CT does not have information about the tumor margins. The RFA electrode was placed by estimating the location of the tumor by using other anatomical landmarks. (c) Aligned pre-procedural MR and intra-procedural CT shows that RFA applicator is not placed accurately. The tumor margin was drawn based on the information provided by pre-procedural MRI.

Image registration has been extensively addressed in the literature. Non-rigid registration is often required in practice. A survey on elastic registration methods for medical images with emphasis on landmark-based schemes has been presented [2].

Several clinical studies have demonstrated the feasibility of rigid registration for prostate and pelvic MR volumes [3], for RF liver ablation based on intra-procedural MRI scanner [4]. Pre-procedural MRI is matched with intra-procedural ultrasound [5] under the assumption of rigid body transformation. A similar approach has been presented [6].

Liver motion and deformation based on gated MR images are modeled [7] based on both rigid and non-rigid registration algorithms. However, execution time is the main limitation for this approach.

Multimodality interventions are feasible by allowing the real-time updated display of previously acquired functional or morphologic imaging during angiography, biopsy, and ablation. However, this entails the use of an electromagnetic tracking device in the interventional room, while the existing instruments need modifications [8].

The utility of enhanced visualization during image guided therapy procedures is clearly demonstrated in the literature. To date, commercial systems can only rigidly align the pre-procedural, high resolution imaging data with the intra-procedural imaging data. However, rigid alignment can result in errors as high as 20 mm. Yet, there has been no fully volumetric, non-rigid registration of liver deformations demonstrated in a clinical environment during interventional procedures.

In this study we assessed retrospectively three different methods for non-rigid registration between pre-procedural MRI and intra-procedural unenhanced liver CT. One was adapted from our previous work on the problem of brain shift. The other two methods are available in open source as part of the ITK (www.itk.org).

Our goal is to establish the feasibility of non-rigid registration for CT guided RF ablation. We measure the accuracy of all three registration techniques, their robustness, and execution time.

2 Material and Methods

2.1 Materials

The study was conducted on 13 retrospective datasets of patients who underwent CT-guided RF ablation of liver tumors (8 metastases and 5 hepatocellular carcinomas - Table 1). For all the patients, the images used are: (1) pre-procedural MR images obtained with a 1.5T MRI (Sigma LX, GE Medical Systems, Milwaukee, WI), matrix=256x256, 1.36 X 1.36 X 2.5 mm. (2) Intra-procedural: Imaging was performed using interventional CT (SOMATOM Plus 4, Siemens Medical Solutions, Erlangen, Germany), matrix=512x512 and voxel size 0.61 X 0.61 X 2.5 mm.

2.2 Methods

Rigid and non-rigid registration

In an initial step, a rigid registration between pre-procedural MRI and intra-procedural CT was performed, based on an ITK implementation of the mutual information.

Three non-rigid registration methods were used. One, introduced by our group [9], and two other standard techniques, available as open-source in ITK: b-splines and demons. In the following sub-section, information about each of these non-rigid registration techniques is presented, together with validation strategy used.

2.2.1 Finite Element Method (FEM) Based

The algorithm we propose is extensively validated on brain MR images. Details are presented in [10] and a brief overview is presented in this section. Recently, this algorithm has been validated on patients enrolled prospectively for image guided neurosurgery [11]. The images used in our study are acquired at the same respiration cycle, therefore the liver deformations are relatively small (up to 20 mm). The linear elastic model previously used [10] can be consequently easily employed for the registration of the liver.

The algorithm can be decomposed into three main parts.

- The first part, in the pre-procedural phase, consists in building the patient-specific liver model utilizing pre-procedural MRI.
- The second part, during the CT guided procedure, is the block matching computation for selected blocks which estimates a set of displacements across the volume.
- The third part, during the procedure, is an iterative hybrid solver that estimates the 3D volumetric deformation field.

Table 1. Details on the RFA patients enrolled in our retrospective study

	Sex	**Age**	**Pathology**	**Location (liver segment)**
Case 1	M	63	Colon metastasis	7
Case 2	F	60	Breast metastasis	7
Case 3	F	55	Ovary metastasis	8
Case 4	F	64	HCC	6
Case 5	F	46	Metastasis from unknown primary	3
Case 6	M	49	Colorectal metastasis	4a
Case 7	F	53	HCC	4a
Case 8	M	60	HCC	6
Case 9	F	75	HCC	4a
Case 10	F	68	colorectal	5
Case11	M	50	Colorectal metastasis	4a
Case12	M	58	GIST	5
Case13	M	60	HCC	2

A key aspect of the deformation estimation is our formulation of the displacement estimation as a continuum between approximation and interpolation strategies. Interpolation strategies ensure that the estimated field exactly matches the displacement identified for each block, but because such matches are noisy, a pure interpolation is prone to error. An approximation strategy does not require the estimated displacement fit exactly each block displacement, and so is better able to reject noise than an interpolation scheme, but is also guaranteed to never exactly recover an estimated displacement which is an undesirable property. In our novel formulation, we first carry out an approximation solution, we then compare the block

displacement with the approximate solution and rank order the blocks according to the magnitude of the difference. We reject outlier blocks that are likely noisy matches by removing the blocks with the largest error. We then re-estimate the displacement utilizing a more stringent approximation criterion, and repeat the procedure. As we increase the strength of the requirement that the approximation solution match the block displacements, we shift from approximating the displacement field to interpolating the displacement field. This makes it possible for us to match exactly the true deformation, which cannot occur with an approximating solution. Furthermore, since we are iteratively rejecting blocks with large displacement error, we are rejecting noisy matches and so we gain robustness to noise and spurious matches that a pure interpolating solution cannot have.

High performance computational architecture

Non-rigid registration algorithms are typically computationally expensive and often proven to be impractical for solving clinical problems. We employed a cluster of computers to achieve near-real time performance. Our implementation addresses three aspects: (1) load balancing, (2) fault-tolerance and (3) ease-of-use for parallel and distributed registration procedures. With dynamic load balancing we improved by 50% the performance of the most computational intensive part, parallel block matching. Our 2-level fault-tolerance introduced a moderate 6% overhead due to additional communication. With web-services and by hiding pre-processing overheads, we developed faster and easier to use remotely registration procedure. Details about the novel technology can be found in [12].

2.2.2 B-Spline Deformable Registration

An ITK-based implementation of the free-form deformation algorithm [13] is used. After affine initialization of the transformation, a displacement field modeled as a linear combination of B-spline is estimated by maximization of the mutual information between the images to be registered. A regular grid of uniformly distributed control points and a gradient descent optimizer were used. A coarse-to-fine pyramidal based approach was employed. At each pyramidal level, both the resolution of the images and the number of control points in each dimension were doubled.

2.2.3 Demons Deformable Registration

An ITK-based implementation of multi-resolution intensity-based algorithm [14] based on the concept of optical flow is used. The image alignment is approached as a diffusion process. The object boundaries in the reference image are viewed as semi-permeable membranes. The moving image is considered as a deformable grid, and diffuses through these interfaces driven by the action of effectors, called demons, situated within the membranes. The smoothness of the displacement field is controlled by filtering at each iteration with a Gaussian function of standard deviation.

2.2.4 Validation of Non-rigid Registration Algorithms

We employ two standard methods for the validation of registration algorithms. The first (i) is an overlap invariant entropy measure of 3D medical image alignment.

The second (ii) is based on an algorithm for extraction of edges of anatomical landmarks. We describe briefly the two validation methods in the following three sub-sections.

(i) Normalized Mutual information (NMI)

NMI is an entropy based measure of alignment between different 3D medical modalities. In practice, direct quantitative measures of information derived from the overlap of a pair of images are affected by local image statistics. In order to provide invariance to overlap statistics, normalized entropy based measure of registration is proposed, which is simply the ratio of the sum of the marginal entropies and the joint entropy. The method was proposed in [15], and used among others by [16].

(ii) Edge distance based

We employ a Canny edge detector to extract edges of the liver and its internal anatomical structures from the CT and MR images. The edges are discretized and represented as a set of points. The 95% Hausdorff distance is measured between the points on the edges extracted from the two images (pre- and intra-procedural). Ideally, when there are no errors in registration present this distance should be 0. The 95% Haussdorff ensures that the outliers are rejected. The method is used in [11].

3 Results

The rigid and non-rigid registration algorithms were successfully applied for all 13 retrospective datasets. The mean execution times were 1 minute for rigid, 10 minutes for b-spline, 6 minutes for demons, and 5 minutes for biomechanical technique. Overall, MI calculations were 0.13 for rigid registration, 0.25 for b-spline, 0.18 for demons, and 0.44 for biomechanical non-rigid registration techniques. The mean distance between the edges of anatomical landmarks of the liver were 12.2 mm for the rigid, 2.4 mm for b-spline, 3.0 mm for demons and 1.64 mm for biomechanical non-rigid registration methods.

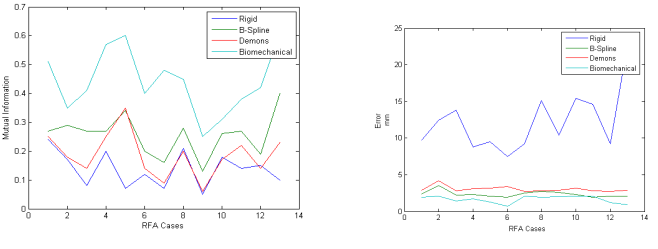

(a) (b)

Fig. 2. The accuracy results for our RFA retrospective study. (a) Mutual information (0-min, 1-max). (b) distance between edges.

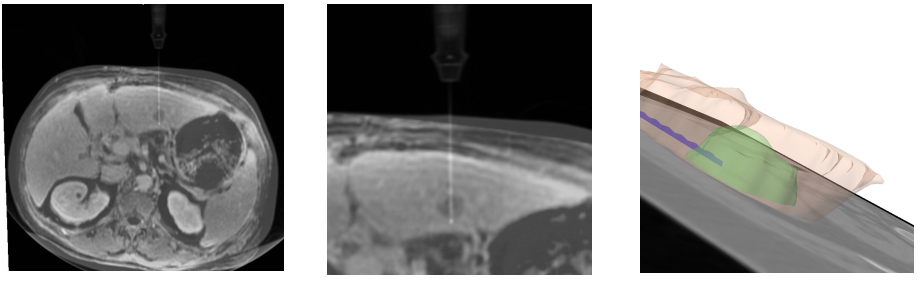

(a) (b) (c)

Fig. 3. Axial images of the same patient as Figure 1. Contrast enhanced pre- MRI overlaid on intra- CT by non-rigid registration (a) and (b). The position of the RFA electrode with respect to the tumor margins can be evaluated in (c).

FEM non-rigid registration technique was significantly better than rigid ($p<10^{-5}$), non-rigid b-spline ($p<10^{-4}$) and demons ($p<10^{-4}$) registration techniques. Details on the accuracy comparison between the three techniques are presented in Figure 2 and Table 2. Examples of registered images with are presented in the Figure 3.

Table 2. Registration results between the pre-procedural MRI and intra-procedural CT images for retrospective data

	Rigid registration between pre-procedural MRI and intra-procedural CT		Non-Rigid registration between pre-procedural MRI and intra-procedural CT					
			B-spline		Demons		Biomechanical	
	Error (mm)	**MI**	Error (mm)	**MI**	Error (mm)	**MI**	Error (mm)	**MI**
Case 1	9.7	**0.24**	2.4	**0.27**	2.9	**0.25**	1.9	**0.51**
Case 2	12.4	**0.17**	3.5	**0.29**	4.2	**0.18**	2.1	**0.35**
Case 3	13.8	**0.08**	2.2	**0.27**	2.8	**0.14**	1.4	**0.41**
Case 4	8.8	**0.20**	2.3	**0.27**	3.1	**0.25**	1.7	**0.57**
Case 5	9.5	**0.07**	2.1	**0.34**	3.2	**0.35**	1.3	**0.60**
Case 6	7.5	**0.12**	1.9	**0.20**	3.4	**0.14**	0.7	**0.40**
Case 7	9.2	**0.07**	2.5	**0.16**	2.7	**0.09**	2.1	**0.48**

Table 2. (*continued*)

Case 8	15.1	**0.21**	2.7	**0.28**	2.8	**0.20**	1.9	**0.45**
Case 9	10.4	**0.05**	2.6	**0.13**	2.9	**0.06**	2.0	**0.25**
Case10	15.4	**0.18**	2.3	**0.26**	3.2	**0.17**	2.1	**0.31**
Case11	14.6	**0.14**	1.9	**0.27**	2.8	**0.22**	2.1	**0.38**
Case12	9.2	**0.15**	2.1	**0.19**	2.7	**0.14**	1.2	**0.42**
Case13	22.5	**0.10**	2.1	**0.40**	2.9	**0.23**	0.9	**0.61**
Avg.	12.16	**0.13**	2.35	**0.25**	3.04	**0.18**	1.64	**0.44**

4 Conclusions

Our study demonstrates that non-rigid registration techniques can be used to register pre-procedural contrast-enhanced MR images with intra-procedural unenhanced CT scans of liver within the time constrains imposed by the RFA procedure and with accuracy found satisfactory by radiologists. Our novel FEM non-rigid registration technique substantially (7 times) improved the accuracy of currently used rigid registration. Our new algorithms is running on a HPC system. Therefore, significant computational resources are required. Nevertheless, it is demonstrated to be fast enough for clinical application, and, achieves better accuracy than the b-spline and demons, for the images used in our study.

For clinical trials, further validation studies are necessary, to assess the accuracy of registration algorithms in the vicinity of tumors. Phantom experiments will be conducted, together with correlation between our prediction outcomes with pathological reports.

The results of our study indicate that this novel technology may be used to optimize placement of applicators during CT-guided RF ablations.

Acknowledgments. This investigation was supported in part by NSF ITR 0426558, and by NIH grants R03 EB006515, U41 RR019703, P01 CA067165, R01 021885.

References

1. Silverman, S.G., Tuncali, K., Morrison, P.: MR Imaging-guided percutaneous tumor ablation(1). Acad. Radiol. 12(9), 1100–1109 (2005)
2. Rohr, K.: Elastic Registration of Multimodal Medical Images: A Survey 14(3) (2000)
3. Fei, B., Duerk, J.L., Boll, D.T., Lewin, J.S., Wilson, D.: Slice-to-volume registration and its potential application to interventional MRI-guided radio-frequency thermal ablation of prostate cancer. IEEE Trans. Med. Imaging 22(4), 515–525 (2003)
4. Carrillo, A., Duerk, J.L., Lewin, J.S., Wilson, D.L.: Semiautomatic 3-D image registration as applied to interventional MRI liver cancer treatment. IEEE TMI 19(3) (2000)

5. Penney, G.P., et al.: Registration of freehand 3D ultrasound and magnetic resonance liver images. Med. Image. Anal. 8(1), 81–91 (2004)
6. Bao, P., Warmath, J., Galloway, R., Herline Jr, A.: Ultrasound-to-computer-tomography registration for image-guided laparoscopic liver surgery. Surg. Endosc. 19(3), 424–429 (2005)
7. Rohlfing, T., Maurer Jr, C.R., O'Dell, W.G., Zhong, J.: Modeling liver motion and deformation during the respiratory cycle using intensity-based nonrigid registration of gated MR images. Med. Phys. 31(3), 427–432 (2004)
8. Banovac, F., Wilson, E., Zhang, H., Cleary, K.: Needle biopsy of anatomically unfavorable liver lesions with an electromagnetic navigation assist device in a computed tomography environment. J. Vasc. Interv. Radiol. 17(10) (2006)
9. Clatz, O., Delingette, H., Talos, I.F., Golby, A.J., Kikinis, R., Jolesz, F.A., Ayache, N., Warfield, S.K.: Robust nonrigid registration to capture brain shift from intraoperative MRI. IEEE Trans. Med. Imaging 24(11), 1417–1427 (2005)
10. Archip, N., Clatz, O., Whalen, S., Kacher, D., Fedorov, A., Kot, A., Chrisochoides, N., Jolesz, F., Golby, A., Black, P.M., Warfield, S.: Non-rigid alignment of pre-operative MRI, fMRI, and DT-MRI with intra-operative MRI for enhanced visualization and navigation in image-guided neurosurgery. Neuroimage (2007)
11. Chrisochoides, N., Fedorov, A., Kot, A., Archip, N., Black, P., Clatz, O., Golby, A., Kikinis, R., Warfield, S.K.: Toward Real-Time, Image Guided Neurosurgery Using Distributed and Grid Computing. In: Löwe, W., Südholt, M. (eds.) SC 2006. LNCS, vol. 4089, Springer, Heidelberg (2006)
12. Rueckert, D., Sonoda, L.I., Hayes, C., Hill, D.L., Leach, M.O., Hawkes, D.: Nonrigid registration using free-form deformations: application to breast MR images. IEEE Trans Med Imaging 18(8), 712–721 (1999)
13. Thirion, J.: Image matching as a diffusion process: an analogy with Maxwell's demons. Med. Image. Anal. 2(3), 243–260 (1998)
14. Studholme, C., Hill, D.L.G., Hawkes, D.J.: An overelap invariant entropy measure of 3D medical image alignment. Pattern Recognition 32(1) (1999)
15. Soza, G., Grosso, R., Nimsky, C., Hastreiter, P., Fahlbusch, R., Greiner, G.: Determination of the Elasticity Parameters of Brain Tissue with Combined Simulation and Registration. Int. J. Medical Robotics and Computer Assisted Surgery (1, Nr. 3)